Desalination and Water Treatment
www.deswater.com

doi: 10.5004/dwt.2018.23084

133 (2018) 292–306
November

Recent progress in the advanced oxidation of wastewaters using recycled fly ashes as alternative catalytic agents

Apostolos N. Baklavaridis[a], Petros E. Samaras[b,*], Vayos G. Karayannis[a]

[a]*Department of Environmental Engineering, Technological Education Institute of Western Macedonia, 50100 Kozani, Greece, emails: abak.stm@gmail.com (A.N. Baklavaridis); vkarayan@teiwm.gr (V.G. Karayannis)*
[b]*Department of Food Technology, Alexander Technological Education Institute of Thessaloniki, 57400 Thessaloniki, Greece, email: samaras@food.teithe.gr*

Received 19 June 2018; Accepted 2 September 2018

ABSTRACT

In this study, a comprehensive literature review is conducted with regard to recent advances in using recycled fly ashes as alternative and cost-effective reagents than as wastes in the advanced oxidation of wastewaters. Fly ashes are powdery solid residues that are produced in enormous quantities in coal/lignite-fed power stations and also from waste incineration. Novel applications of these industrial by-products in the field under examination, toward sustainable use of resources and circular economy, are discussed and summarized. Since fly ashes contain useful metal oxides, they can actually be considered as alternative catalytic agents in wastewater treatment, depending on their surface properties and the elements solubility rate in the aqueous media. Beyond the possible contribution of these secondary materials to the oxidation of wastewaters, their potential for concurrent beneficial adsorption of substances present in the effluent to be treated also enhances the significance of the current scientific work. For that purpose, fly ashes and several fly ash-based composite catalysts were examined for their effectiveness in advanced oxidation processes that are summarized in three main categories, namely photocatalysis, Fenton/Fenton-like oxidation, and combined mechanisms. Principal system parameters affecting the degradation of wastewaters were considered, including the dosage of each catalytic agent used, the initial dye concentration, the solution pH, and the reaction time and temperature.

Keywords: Wastewater; Advanced oxidation; Photocatalysis; Fenton; Fly ash; Valorization; Catalyst

1. Introduction

Wastewaters contain in many cases harmful and/or toxic pollutants that pose serious environmental issues. These pollutants are often present in various types of effluents, such as municipal, pharmaceutical, textile, and chemical industry wastewaters. Most common compounds found include pharmaceutical (e.g., cephalexin, levofloxacin, and pentoxifylline (PEN)), organic compounds (e.g., phenols, dioctyl phthalate (DOP), and dichloroacetic acid), and textile (azo) dyes (e.g., methylene blue (MB), Rhodamine B (RhB), and acid orange 7 (AO7)). The degradation of pollutants with poor biodegradability is an important challenge nowadays. In that sense, various research efforts are destined toward to the development of facile, efficient, and environment-friendly methodologies for wastewater treatment [1–6].

Advanced oxidation processes (AOPs) represent a promising category of wastewater treatment methodologies that have to do with the complete decomposition (degradation) of dangerous pollutants into inert and nontoxic derivatives. In general, this is realized by the in-process production of reactive species, such as free hydroxyl radicals ($^{\bullet}$OH), superoxide

---

* Corresponding author.

Presented at the 6th International Conference on Environmental Management, Engineering, Planning and Economics (CEMEPE-2017), 25–30 June 2017, Thessaloniki, Greece.

anion radical, hydrogen peroxide, and singlet oxygen. All of the aforementioned reactive species have a quite strong oxidation potential, and, consequently, enhanced ability to oxidize the pollutants. Certainly, hydroxyl radical is the dominant and most efficient reactive radical in advanced oxidation. Organic pollutants generally interact with $^{\bullet}OH$ via either the subtraction or the addition of hydrogen. In this way, a carbon-centered radical occurs. Subsequently, this radical reacts with molecular oxygen, forming a peroxyl radical that further reacts toward oxidation products such as alcohols, aldehydes, or ketones. Alternatively, $^{\bullet}OH$ may form a radical cation by subtracting an electron from various electron-rich substrates. This can immediately hydrolyze in aqueous media, yielding an oxidized product. The oxidation products are often less toxic and more susceptible to bioremediation toward CO_2, water, etc. AOPs can be categorized in three main categories, depending on the advanced oxidation mechanism used: (1) photocatalysis (UV/TiO_2, UV/H_2O_2, $UV/TiO_2/H_2O_2$), (2) Fenton and Fenton-like, and (3) alternative and combined mechanisms (photo-Fenton, nonthermal plasmas, sonolysis, radiolysis, etc.). Generally, AOPs' efficiency depends on the specific method applied, the physicochemical properties of the pollutant, and the operating parameters/conditions. In terms of practical applications, advanced oxidation is used in industry, hospitals, and wastewater treatment plants. AOPs have low installation costs but they have relatively high operating costs. This is due to chemicals and energy requirements [7]. In order to limit these drawbacks, AOPs are commonly employed as a pretreatment in combination with a biological treatment. Moreover, the combination of various AOPs procedures is a rather efficient way to reduce operational costs and to enhance the pollutant removal efficiency [7–10].

AOPs have attracted much attention lately not only by the global research community [9–13], but also by our research group [14–17]. The increasing interest related to the advanced oxidation of wastewaters is illustrated by the increasing number of publications over the last 15 years, as shown in Fig. 1.

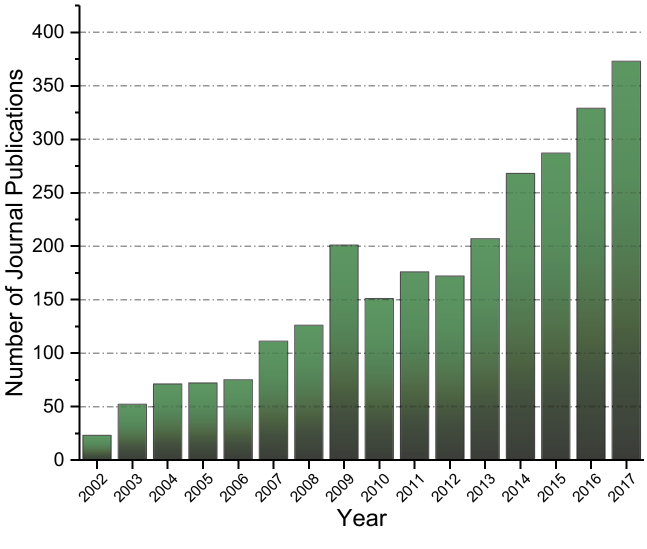

Fig. 1. Journal article results from the last 15 years using *Scopus*, using the keyword "advanced AND oxidation AND wastewater."

Up to now, various catalytic materials/systems have been tested with regard to their effectiveness in AOPs. For instance, Fe(III)/TiO_2-montmorillonite photocatalyst was tested in a photo-Fenton-like process [18], while TiO_2/Ti electrodes were used in a photocatalytic process [19]. Furthermore, in the framework of circular economy, using waste to treat various types of wastewater is gaining attention. Interestingly, fly ash (FA), coming from various sources, such as coal/lignite power plants, waste and agricultural products incineration, seems to have many advantages for its usage in AOPs: high availability, different surface chemistry (Ca or Si), high surface area, high absorption capacities, and low cost. In that sense, various systems using FA were fabricated and applied to AOPs [20–22].

In this work, recent advances in employing recycled FAs and ash-based composites as substitute and cost-effective reagents than as wastes in wastewater treatment are reviewed and summarized, in order to assess their potential for use in viable and efficient remedial alternatives to conventional procedures.

Our literature review was based on 64 selected journal articles from the last 5 years. Their distribution is shown in Fig. 2.

2. FA-based advanced oxidation of wastewater

Various advanced oxidation mechanisms have been proposed using FA-based catalytic materials. These mechanisms may be summarized in three main categories: photocatalysis, Fenton/Fenton-like, and combined mechanisms.

2.1. Photocatalytic oxidation

In various studies, researchers attempted the photocatalytic removal of organic pollutants:

Giri Babu et al. [23] studied four different FAs as a catalyst for the degradation of Acid Red 1 using UV irradiation.

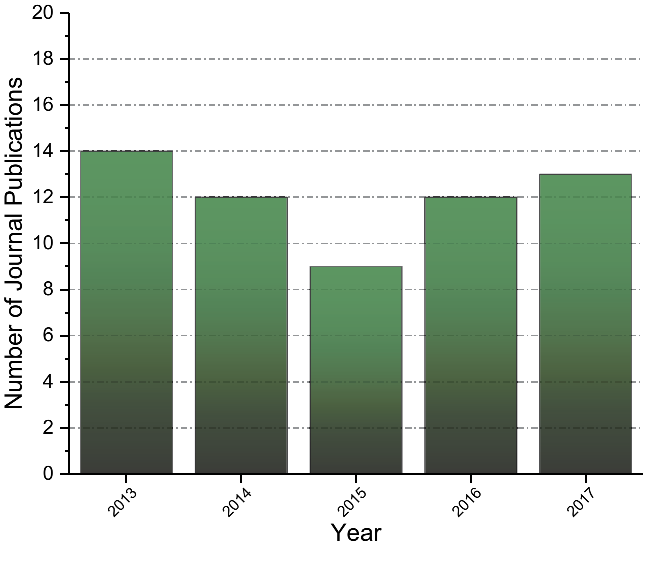

Fig. 2. Selected articles used in this study based on *Scopus* search using "fly ash based advanced oxidation wastewater" keyword, from years 2013 to 2017. One publication was included from 2018.

These FAs were collected from different thermal power stations located at various places in India and having different chemical compositions. Three of them were from lignite-based thermal power plants and one from a coal-fed power plant. One FA is classified as Class F, two as Class C and the other one is not conforming to ASTM C618 classification. In 60 min duration, the dye degradation efficiency at optimal parametric values of pH 2.5, initial dye concentration of 10 mg/L, and catalyst dosage of 1.0 g/L using various FAs, that is, from Salam Power Plant, Barmer Lignite Power Plant, Kutch Lignite Power Plant, and Neyveli Lignite Thermal Power (NLTP) plant were found to be 40%, 60%, 67%, and 95%, respectively. The contribution of adsorption alone was 18% at the above-mentioned optimal conditions. Among the above four FAs, the NLTP one was proved to be most efficient.

In advanced oxidation of wastewaters via photocatalysis employing FAs as alternative catalytic agents, the foremost catalyst used is FA/TiO_2. Malakootian et al. [24] used a photocatalytic process as a suitable method for *o*-chlorophenol removal. Specifically, they studied the photocatalytic efficiency of FA modified with TiO_2 nanoparticles in the removal of *o*-chlorophenol. The removal efficiency using a composite catalyst composed of modified FA and TiO_2 reached 98.9%, while the removal efficiency by TiO_2/UV without using FA was 78.7%. In another work, Andronic et al. [25] developed materials with photocatalytic and adsorption properties for advanced wastewater treatment, targeting reuse. Making use of TiO_2 as a well-known photocatalyst, Cu_2S as a Vis-active semiconductor, and FA as a good adsorbent, dispersed mixtures/composites were prepared to remove pollutants from wastewater. Experiments using the new catalysts were carried out both at laboratory scale (in two solar simulators) and real scale. The radiation intensity was shown to significantly affect the phenol degradation rate. The composite mixture of TiO_2 and FA is two to three times less active than sol–gel TiO_2. Photodegradation kinetic data on the highly active TiO_2 were compared for pollutant elimination. Photodegradation of dichloroacetic acid was fast and complete after 90 min in real scale, while after 150 min, imidacloprid and phenol removal was 90% and 56%, respectively. Moreover, Shi et al. [26] developed a new type of composite photocatalyst TiO_2/CFA by hybrid slurry procedure. The increase of catalyst loading improved the photocatalytic activity of TiO_2/CFA. Nevertheless, during the wastewater treatment procedure, superfluous TiO_2 grains broke easily away from CFA when the loadings were too high. This is not favorable for TiO_2/CFA photocatalyst reuse. The optimal loading of TiO_2 was about 50%. Degradation efficiency was maintained above 70% without any decrease when the composite photocatalyst was reused for up to six times.

Other studies refer to the production and testing of nanocomposite TiO_2/FA photocatalysts. Visa et al. [27] reported the synthesis, characterization, and adsorption properties of a novel nanocomposites obtained using the hydrothermal method. Specifically, nanocomposites were produced by combining FA-TiO_2 slurry and a surface modifier, hexadecyltrimethylammonium bromide (CTAB). The advanced (photocatalytic) oxidation properties of the nanocomposites were tested in multipollutant synthetic wastewaters loaded with copper cations and two industrial dyes (acid dye Bemacid Blau and reactive dye Bemacid Rot). The nanocomposite catalyst achieved high removal efficiencies of more than 90%, both in adsorption and in photodegradation experiments, in optimized conditions. In another work of Visa et al. [28], a TiO_2-FA composite was developed based on interaction of the constituents in alkaline solution via low-temperature hydrothermal methods, in order to obtain nanocomposite catalysts. By combining FA with TiO_2, the following advantages appeared: (1) the TiO_2 crystallites grew on the support (active FA); (2) pollutant molecules migrated to the surface of TiO_2 and then were degraded by photocatalysis; and (3) activated FA substrates were regenerated in situ. The photocatalytic property of the composites was evaluated by MB and surfactant (dodecylbenzenesulfonate) degradation under UV and visible irradiation. The adsorption tests were made on heavy metal (Cu^{2+}) cation. Properties of composites were correlated with the adsorption/photocatalytic activity of the samples.

Some other studies are dedicated to the utilization of different forms of nano-TiO_2 in FA/TiO_2 nanocomposite catalysts. Saud et al. [29] prepared FA-doped TiO_2 nanofibers by electrospinning process for the removal of organic pollutant and microorganism from water. Calcination of electrospun nanofiber mats composed of titanium tetraisopropoxide, poly(vinylpyrrolidine) and FA in air at 600°C led to creation of good morphology FA/TiO_2 nanofiber. In fact, synthesized nanofibers revealed a distinct performance in adsorption and photocatalytic activity for decomposition of MB, and antibacterial activity against *Escherichia coli*, due to combined effect of TiO_2 and FA. Results indicated that as-synthesized composite nanofibers exhibit great potential for water purification. Furthermore, in order to address the problem with titania distribution and recovery, Cui et al. [30] fabricated a series of $Ti_{0.91}O_2$/CFA photocatalysts ($Ti_{0.91}O_2$/CFA-*n*, *n* = 2,4, 6, and 8) by assembling $Ti_{0.91}O_2$ nanosheets on coal fly ash (CFA) microspheres, via the layer-by-layer assembly (LBLA) process. By the LBLA procedure, $Ti_{0.91}O_2$ nanosheets were successfully immobilized on the CFA. In this way, a notable change in the CFA characteristics was observed. The photocatalytic activity of $Ti_{0.91}O_2$/CFA was evaluated by MB photodegradation, under UV irradiation. The best photocatalytic activity was achieved in the $Ti_{0.91}O_2$/CFA sample that was irradiated for 60 min, having a decolorization rate above 43%. After photocatalytic procedure, $Ti_{0.91}O_2$/CFA could be easily separated and recycled from aqueous solution. $Ti_{0.91}O_2$ nanosheets were shown to be still anchored on the CFA.

Several studies also utilize an additional photocatalytic constituent in order to enhance the activity and efficiency of FA/TiO_2 (nano)composite catalysts. In that sense, more sophisticated photocatalytic systems were produced. In a recent study, Fan et al. [31] investigated various activated fly ash cenosphere (AFAC) supporting TiO_2-coated $ZnFe_2O_4$ (TiO_2/$ZnFe_2O_4$/AFAC) photocatalysts, prepared by sol–gel and hydrothermal methods. They found that the main components of spherical AFAC were mullite ($Al_6Si_2O_{13}$) and SiO_2. Moreover, the crystallite size of the TiO_2/$ZnFe_2O_4$ nanocomposite was less than 10 nm and its specific surface area was 162.18 m^2/g. The TiO_2/$ZnFe_2O_4$ nanocomposite had a bandgap of 2.56 eV, which would photodegrade 95% of RhB under visible light within 75 min. When hybridized with 0.02 g AFAC, the TiO_2/$ZnFe_2O_4$/0.02 g AFAC photocatalyst with a bandgap of 2.50 eV could remove 97.1% of RhB and be reused three consecutive times with minor decrease in photocatalytic performance. However, the photocatalytic efficiency decreased to 91.0% on increasing the dosage of AFAC to 0.30 g. The mesoporous structure of all photocatalysts and the strong adsorption ability of AFAC contributed to the notable performance. Furthermore, Zhao et al. [32] produced ternary photocatalysts using an in-situ hydrolysis procedure, toward stability and photocatalytic efficiency enhancement. These catalysts were composed of g-C_3N_4/N-TiO_2/FACs. When TiO_2 was anchored on FAC, it was easily to be separated from the aqueous solution. In this way, it could be repeatedly utilized. The degradation rate was more than 68% even after seven times photocatalyst reuse. The synergistic effect between N-TiO_2 and g-C_3N_4 could be reflected to the bandgap values of 2.75 eV of the g-C_3N_4/N-TiO_2/FAC catalyst. The composite of g-C_3N_4/N-TiO_2/FAC had an ideal photocatalytic activity of 72.2% under visible light for 180 min. It was about 1.3 times of N-TiO_2/FAC and 3.5 times of g-C_3N_4. The improvement of the photocatalytic effectiveness could be attributed to the synergistic effect of SiO_2, Fe_2O_3, and TiO_2 constituents. In another study, Yang et al. [33] prepared HPW-CS/TiO_2/FACS photocatalysts for degradation of tetracycline (TC) hydrochloride. Specifically, they used molecular imprinting technology in combination with photodegradation technology to synthetize HPW-CS/TiO_2/FACS photocatalysts. The novel photocatalyst could not only exhibit high photocatalytic activity but also be easy to reuse, because the fly ash cenospheres (FACs) were adopted for carrier. The compound photocatalyst was characterized by various analytical techniques. Meanwhile, the effects of the amount of heteropolyacid, dosage of chitosan (Cts), and calcination temperature on the photocatalytic activity of the photocatalyst were investigated. Moreover, Hou et al. [34] used floating solid FACs as the carrier to prepare Ag_3PO_4/$ZnFe_2O_4$/FACs composite materials using sol–gel and liquid phase deposition methods. The material photocatalytic activity was studied in visible light using MB as the goal pollutant. Compared with single powder catalysts, Ag_3PO_4/$ZnFe_2O_4$/FACs composites had the highest photocatalytic efficiency and could float in water, because FACs are lightweight and hollow. Furthermore, the composite materials can absorb high amounts of light energy and are conducive for catalyst recycling and reuse. Recycling experiments demonstrated that the Ag_3PO_4/$ZnFe_2O_4$/FACs catalyst retained high photocatalytic activity after five times of recovery. In another study, Liu et al. [35] developed a cube-like Ag@AgCl-doped TiO_2/FAC composite (denoted Ag@AgCl–TiO_2/FACs) that was successfully synthesized via a two-step approach. The RhB photocatalytic degradation rate with Ag@AgCl–TiO_2/FACs was 1.56 and 1.33 times higher than that with AgCl–TiO_2/FACs and Ag@AgCl, respectively. The RhB degradation rate with Ag@AgCl–TiO_2/FACs was nearly 100% within 120 min under visible light. Analysis of active species indicated that O_2 and h+ dominated the reaction, and OH participated in the photocatalytic reactions as an active species. A mechanism for the photocatalytic degradation by the Ag@AgCl–TiO_2/FACs was proposed based on the experimental results. Moreover, Fan et al. [36] prepared V-doped TiO_2/FAC photocatalytic composite materials by sol–gel method with FAC as a carrier, tetrabutyltitanate as titanium source, and ammonium metavanadate as vanadium source. The photocatalytic activity of the samples was studied using degradation of dimethylformamide (DMF) as organic pollutant. The TiO_2 loaded on FAC surface was found to be anatase. It was also shown that doped V exists in the form of V^{4+} and V^{5+} in the TiO_2 lattice, and that the doping of V could promote TiO_2 response to visible light (red shift) and improve the photocatalytic activity of the catalyst. However, excessive V doping would lead to the decrease of photocatalytic activity. It was determined that when the optimum doping amount of V is 1% and the dosage is 0.5 g, the removal rate of DMF solution with the concentration of 50 mg/L and pH = 3 reaches 88.2%, after 30 min dark reaction and 180 min photocatalysis. Interestingly, the degradation rate of DMF solution still remains above 65% even in the fourth reuse cycle, which shows good photocatalytic activity and stability. In another study, Zhao et al. [37] successfully synthesized V-TiO_2 FACs by sol–gel method. The V-TiO_2/FA catalyst was found to mainly preserve its anatase phase after calcination at 500°C. The photocatalytic activity was evaluated by the degradation of Direct Fast Scarlet 4BS under UV light. The degradation rate of V-TiO_2/FA was higher than that of TiO_2/FA, and reached up to 98.7% after UV irradiation for 90 min. Therefore, the V-TiO_2/FA catalyst prepared appeared to possess enhanced photocatalytic properties. Furthermore, Wang et al. [38] developed novel photocatalysts consisting of TiO_2-coated hydroxylated FACs by using a sol–gel procedure. For further formation of Pt-TiO_2 films (PTF) supported on hydroxylated FACS photocatalyst, Pt was deposited on these TiO_2/FAC particulates, via photoreduction. The photocatalytic activity of PTF was evaluated via MB photodegradation. The best photocatalytic activity for MB decomposition was achieved via calcination at 450°C and 1.5% Pt/TiO_2 mass ratio and with 3 g/L catalyst concentration. The MB photodegradation by PTF in aqueous solution was more efficient at rather alkaline conditions. Moreover, the addition of anions in relatively small concentrations improved the photocatalytic efficiency of PTF, due to the improvement of MB adsorption. Nevertheless, this effect appeared to be weakened as the anion concentration was increased. Regarding the catalyst recycling tests, calcination of the used PTF contributed to the photocatalytic activity regain. Furthermore, Duta and Visa [39] successfully produced hydrothermally a ternary composite catalyst consisting of FA, TiO_2, and a cationic surfactant. The photocatalytic activity and efficiency of this novel composite catalyst was evaluated in the removal of Bemacid Red (BR) and Bemacid Blue (BB) dyes in alkaline conditions (pH ~ 10.6). The adsorption effectiveness was shown to be strongly dependent on the substrate micropores characteristics. Photodegradation efficiency was 77% for BB and 93% for BR after 240 min under UV irradiation. Additionally, Huo et al. [40] prepared porous-TiO_2/FAC photocatalysts via sol–gel with a traditionary surfactant CTAB as template. The as-prepared porous photocatalysts were further modified by poly-*o*-phenylenediamine (PoPD) with photo-induced method. The photocatalytic activity was investigated via degradation of ciprofloxacin (CIP) antibiotic wastewater under visible light. The porous structure appeared to be well formed on the surface of TiO_2/FACs, and photocatalytic activity was apparently enhanced with modified PoPD. The degradation of CIP with PoPD/

porous-TiO_2/FACs could reach 71.36%, being improved by about 36% compared to that with TiO_2/FACs as the photocatalyst. Thus, it was clearly shown that the properties of porous microstructure and PoPD modification could effectively increase the photocatalytic activity. Moreover, Song et al. [41] reported the development of a novel composite photocatalyst, composed of carbonized Cts and Fe-N-codoped TiO_2 floating catalyst (layer-by-layer) that was supported on FACs. A rather simple sol–gel method was used for the photocatalyst preparation. The Fe-N codoping lead to bandgap constriction, while the carbonized Cts layer increased the adsorption capacity of the photocatalyst and also its visible light absorption capability. Both photocatalysts, Fe-N-TiO_2/FAC and N-TiO_2/FAC, exhibited excellent performance in RhB photodegradation. Specifically, the RhB photodegradation efficiency of Fe-N-TiO_2/FAC-Cts, measured after 240 min under visible light, was found to be approximately 1.5 and 2.09 times higher than that of Fe-N-TiO_2/FAC and N-TiO_2/FAC, respectively. It was also shown that the floating photocatalyst may be reused up to three times without any notable decrease on RhB photodegradation effectiveness. Yu et al. [42] immobilized transition metal ions on TiO_2/FACs with PoPD. The photocatalytic activity of M-POPD/TiO_2/FACs was studied in the degradation of TC, oxytetracycline (OTC), CIP, TC hydrochloride, and chloromycetin, in simulated wastewater under visible light. M-POPD/TiO_2/FACs could effectively increase the separation rate of photoelectrons and holes in the cycling system and improve the photocatalytic activity for the degradation of antibiotics. The as-prepared M-POPD/TiO_2/FACs were more suitable for TC degradation that reached 71.7%. In another work, Lu et al. [43] prepared a novel photocatalyst by using TC as the molecular template and POPD/TiO_2/FACs as support. In this way, the molecularly imprinted photocatalyst (MIP) possessed the specific recognition ability toward TC, was synthesized via the surface imprinting technology and the photo-induced method, and had hollow spherical structure. Its photocatalytic activity was evaluated by degrading 20 mg/L TC solution under visible light, and photodegradation could reach 77%. In addition, MIP showed the strong ability to selective recognition and photodegradation of TC in the ternary solution containing TC, OTC, and CIP. The coefficient of selectivity ($k_{selectivity}$) of degradation of TC relative to OTC and CIP was 1.67 and 1.25, respectively. Study of the TC photodegradation mechanism indicated that TC was degraded step by step and finally decomposed to CO_2, H_2O, and other gaseous components. Moreover, Lv et al. [44], prepared nano-TiO_2/FA beads composites by hydrolysis-precipitation method, using $TiCl_4$ as the titanium source and urea as the precipitating agent. With the use of $(NH_2)_2CO$ and $(NH_2)_2SC$ as the N and S source, respectively, N and S codoped TiO_2/FA beads composite materials were elaborated by grinding them together according to a certain proportion and calcined at 500°C for 2 h. The UV–Vis absorption spectra showed that the absorption edge of undoped composites is 390 nm, while that of doped composites red-shifts to 500 nm. The photocatalytic activity of the composites was evaluated by degradation of methyl orange (MO) under visible light. After irradiation for 1 h, the degradation rate with N, S codoped-TiO_2/FA beads composite material can reach 65%, while the degradation of undoped sample and P25 were just 10% and 6%, respectively. The composite also showed excellent recycling properties.

Some works report the production of novel FA-based photocatalysts by combing FA with Zn- and Cd-based oxides and sulfides (e.g., ZnO, ZnS, and CdS). One work of Kalpana and Selvaraj [45] investigated the production of a ZnS enwrapped amine functionalized FA nanocomposite photocatalytic system (ZnS/A-FA) via a wet chemical route. The nanocomposite system photocatalytic activity was evaluated via MB degradation, under UV, and for catalyst concentrations up to 3%. ZnS supported by FA showed improved photocatalytic activity compared with that of pristine ZnS. Moreover, from the antibacterial studies, it was concluded that ZnS enwrapped A-FA catalyst provides better antibacterial properties than that of pristine A-FA and ZnS nanoparticles. In another work of Kalpana and Selvaraj [46], a novel nanocomposite system consisting of ZnS/SnS/A-FA was produced for the removal of both dye molecules and pathogenic bacteria. By using $ZnNO_{36}H_2O$, $SnCl_{22}H_2O$, A-FA, and Na_2S as precursors, this novel catalyst was developed at ambient temperature. The results shown that the FA when combined with ZnS/SnS, can degrade the congo red dye within 150 min, by employing low photocatalyst loadings (10 mg). The photocatalyst ability for reuse was also tested; ZnS/SnS/A-FA was rather stable during reuse experiments. Furthermore, the antibacterial properties of ZnS/SnS/A-FA were investigated in both gram-negative bacteria (*E. coli*) and gram-positive ones (*Staphylococcus aureus*). The results shown a significant antibacterial activity of ZnS/SnS/A-FA compared with ZnS/A-FA. Moreover, Kim et al. [47] developed a quite stable Ag-doped ZnO/FA composite photocatalyst via a hydrothermal procedure. FA was used as a support surface for in situ Ag and ZnO nanoparticle deposition, while treating hydrothermally. This led to a particle size decrease and, subsequently, to a surface area increase. The nanocomposite photocatalyst antibacterial activity and photocatalytic efficiency were evaluated using *E. coli* and MB respectively, under UV irradiation. The nanocomposite photocatalyst exhibited a high photocatalytic efficiency and bacterial removal capacity, as well as good reusability.

Other innovative research works demonstrate the applicability of magnetic (nano)particles to the production of novel photocatalytic systems. He et al. [48] developed a magnetic photocatalyst via chemical deposition. Specifically, the catalyst was developed by directly growing photocatalytic nanoparticles (CdS) on the surface of magnetic fly ash cenospheres (MFACs). The photodecomposition results of danofloxacinmesylate indicated a much higher photocatalytic activity of CdS/MFACs (76.2%) than that of pure CdS (71.5%), under visible light. The authors attributed the improved photodegradation of danofloxacinmesylate to photogenerated holes and $^{\bullet}O_2^-$. The photocatalyst exhibited rather good stability and reusability even after five cycles. In another work, Lu et al. [49] reported the production of a TiO_2 photocatalytic system by using a magnetic FA-based composite as support via a sol–gel procedure. This magnetic composite was prepared by coating a special layer of macromolecule onto the surface of the floating carboxyl-functionalized FACs via microemulsion process, and magnetic Fe_3O_4 nanoparticles were introduced into the special layer of macromolecule. The produced photocatalyst not only showed a significant catalytic efficiency but also increased stability. Specifically, the enrofloxacin hydrochloride residues photodegradation efficiency could reach 75.32%, after 60 min under visible light. Moreover, the inorganic salts presence and the varying calcination temperatures were found to have a significant effect on the enrofloxacin hydrochloride photodegradation.

Some works are destined toward the development of photocatalysts based on Bismuth (Bi) oxides. Lin et al. [50] successfully produced three-dimensional (3D) hierarchical microspheres. These microspheres consisted of BiOBr/BiOI deposited on the FACs surface, by a one-pot solvothermal procedure. The loaded hierarchical microspheres exhibited a uniform distribution, while some minor aggregation was also observed. These hierarchical microspheres consisted of two-dimensional (2D) nanosheets, which formed heterojunctions. The photocatalytic activity of the produced ternary composite photocatalyst (BiOB/BiOI/FACs), evaluated in RhB decomposition under visible light, was superior to that of the binary photocatalysts (i.e., BiOI/FACs and BiOBr/FACs). In other work, Zhang et al. [51] successfully synthesized a composite photocatalyst (CeO_2–$BiVO_4$/FAC), by combining impregnation and modified metalorganic decomposition (MOD) procedures, upon visible light irradiation. Specifically, CeO_2–$BiVO_4$ was formed photocatalytically on FACs. The composite catalyst exhibited enhanced photocatalytic activity for MB degradation under visible light. Especially, the photocatalyst with the highest photocatalytic efficiency for MB degradation was the one with 7.5 wt. % CeO_2–$BiVO_4$/FAC. In another work of Zhang et al. [52], a novel $BiVO_4$/FACs composite photocatalyst was developed by the modified MOD method. The photocatalytical activity under visible light and the adsorption parameters were evaluated using the MB dye. FACs were used as supports in order to improve the photocatalytic activity and adsorption of $BiVO_4$. In fact, the composite photocatalyst $BiVO_4$/FACs showed improved photodegradation efficiency and adsorption capacity, which were approximately double compared with those of pure $BiVO_4$. Moreover, recovery tests have shown that $BiVO_4$/FACs were quite stable during the MB photodegradation. In a third work of Zhang [53], novel photocatalytic composites (Pt–$BiVO_4$/FACs) were produced by the aforementioned MOD process and a subsequent photochemical reduction step. In this way, FACs supported Pt–$BiVO_4$ was produced. The results indicated enhanced photocatalytic efficiency of the Pt–$BiVO_4$/FACs system in MB photodegradation under visible light. It is worth noting that the 2 wt. % Pt-loaded photocatalyst exhibited the highest photocatalytic efficiency.

Furthermore, the formation of suitable FA-based geopolymeric systems was even proposed, for application in wastewater advanced oxidation. In particular, Zhang and Liu [54] successfully produced a geopolymer from alkali-activated FA, exhibiting two main nanofeatures: it is composed of nanoparticles with 50 nm average diameter and its porosity lies in the nanoscale, with a quite large pore volume fraction (90%) sized 17–700 nm. The evaluation of this novel catalyst in MB degradation using UV irradiation revealed the synergistic effect of semiconductor photocatalysis and adsorption, which led to photodegradation efficiencies for MB up to 92.79%.

2.2. Fenton and Fenton-like oxidation

Various studies demonstrate the applicability of the Fenton process in wastewater treatment:

Pang et al. [55] focused on treatment of wastewater deriving from phenolic resin production units. This type of wastewater contains formaldehyde and phenol in high concentrations. A combined treatment process was therefore employed, comprising Fenton oxidation (i.e., a secondary condensation), sand filter, and CFA adsorption. It is worth noting that the feasibility of this procedure was illustrated by some successful results in practical operation. Particularly, the out-sourcing water from the treatment facility successfully reached the first order of Integrated Wastewater Discharge Standard (GB 8978-1996). Additionally, some phenolic resin quantities were also recovered, after wastewater treating with this method. In another study, Wang et al. [56] combined FA and Fenton reagent for DOP wastewater treatment. They studied the effect of FA loading, H_2O_2 and Fe^{2+}concentration, pH, as well as other factors, on COD (chemical oxygen demand). The synergistic effect of both Fenton reagent and FA on the COD removal efficiency was found to be superior compared with that recorded for the Fenton reagent alone. Specifically, the maximum COD removal efficiency was approximately 83%, for Fe^{2+} concentration of 1.0 g/L, H_2O_2 concentration of 1.2 g/L, pH = 5 and FA dosage of 4 g. Furthermore, Duc [57] used modified FA for the degradation of Reactive Blue 181 via the heterogeneous Fenton reaction. The novel catalysts were produced via incipient impregnation, employing iron(III) nitrate to support the metal. The influence of advanced oxidation parameters, including H_2O_2 concentration, catalyst dosage, and pH, on the degradation efficiency was studied. The suitability of the heterogeneous Fenton method for Reactive Blue 181 removal from aqueous solution by using modified FA/H_2O_2 was shown. Degradation efficiencies of approximately 90% were recorded using optimal parameters: processing duration 90 min, pH = 3, H_2O_2 concentration of 3.92 mM, and catalyst dosage of 0.4 g/L.

Moreover, several studies investigate the applicability of modified Fenton process (i.e., Fenton-like) to the advanced oxidation of wastewaters. Wang et al. [58] studied the performance of acid-modified CFA for use as a catalyst of a Fenton-like process in *p*-nitrophenol (*p*-NP) wastewater treatment. Particularly, HNO_3-modified fly ash (HFA) had a better catalytic capacity (96.6% *p*-NP removal rate) than those (<92% *p*-NP removal rate) of CFA modified by other acids (HCl, H_2SO_4, and H_3PO_4). The *p*-NP removal rate that is attributed to HFA adsorption was found to be not significant (<3%) compared with the removal rate that is due to the advanced oxidation procedure. *p*-NP degradation efficiencies of 98% were recorded by using the optimal experimental conditions: 10.0 g/L CHFA loading, 170 mg/L CH_2O_2 concentration, 150 rpm agitation speed, pH = 2, 25°C temperature, and 60 min processing time. Moreover, HFA exhibited superb reusability and catalytic stability, as *p*-NP degradation efficiency was found to be higher than 91%, after reusing nine times. In another study, Wang et al. [59] investigated the CFA modification for the production of three different heterogeneous Fenton-like catalysts: granular MCFA (modified CFA), MCFA powder, and Fe_2O_3/granular MCFA.

The catalytic efficiency was found to depend on the specific CFA type used. Specifically, the acid modification was proved to offer much better CFA activation, yielding to *p*-NP degradation efficiencies up to 64%, compared with alkali and heat modification that lead to lower degradation efficiencies up to 45%. Regarding the granular MCFA catalyst, attapulgite was found to better enhance MCFA powder bonding, compared with kaoline. Furthermore, the efficiency of granular MCFA was shown to significantly increase by producing MCFA-supported Fe_2O_3 catalysts. Reusability tests revealed that the three types of MCFA catalysts produced may be reused more than three times, with COD removal rates of 57%. In a third work of Wang et al. [60], a H_2SO_4-modified FA catalyst was developed for phenol wastewater treatment. The operating parameters were determined by single-factor experiments and their significance assessment was conducted, and also the combination of the factors was optimized using an orthogonal experimental design. The significance of the treatment procedure factors, with increasing order was found to be: modified FA dosage < pH < phenol initial concentration < H_2O_2 dosage < $FeSO_4$ dosage. The optimized factor values were: modified FA dosage of 200 mg/L, pH = 5, phenol initial concentration of 300 mg/L, 3 wt. % H_2O_2 dosage of 7 mL, and 5 wt. % $FeSO_4$ dosage of 1 mL. Under these optimized conditions, phenol degradation efficiency reached 99.46%. Furthermore, Dao et al. [61] used an iron-impregnated FA (Fe-FA) as a Fenton-like effective heterogeneous catalyst for Reactive Blue 182 (RB182) decomposition in aqueous solutions. Effects of some key operating parameters, such as (1) dose of H_2O_2, (2) catalyst dosage, (3) pH, and (4) temperature, on the decolorization efficiency were investigated and discussed. Under optimal conditions, a 93% degradation efficiency was recorded in 50 min. Moreover, Fe-FA had good reusability and stability. Kinetic studies indicated that RB182 decolorization by using Fe-FA catalyst matches that of a typical pseudo-first-order reaction with 15.2 kJ/mol activation energy. Duc et al. [62] removed Reactive Blue 19 dye from aqueous solutions by an heterogeneous Fenton-like process also using Fe-modified FA. Under the suitable conditions including catalyst dose of 0.6 g/L, H_2O_2 dose of 4 mM, and pH = 3, the RB19 degradation efficiency attained 92% and 97% in 6 and 24 h, respectively. The catalyst could be reused without reduction of degradation performance. Moreover, Chen and Du [63] degraded *n*-butyl xanthate from aqueous solutions, using FA as a catalyst in a Fenton-like oxidation procedure. The effect of various parameters on the degradation efficiency of the oxidation procedure was investigated. Both the initial solution pH and the catalyst dosage affected significantly the degradation efficiency of *n*-butyl xanthate. A 97% *n*-butyl xanthate degradation efficiency and more than 96% COD removal efficiency could be achieved by using FA as heterogeneous catalyst in optimized conditions (120 min treatment time, pH = 3, FA dosage of 1.0 g/L, H_2O_2 concentration of 1.176 mmol/L, and 4.14 wt. % Fe(III) oxide).

Various studies demonstrate the applicability of Fenton or Fenton-like oxidation processes also to standard wastewater treatment processes. Zhuang et al. [64] employed a novel integrated process, with heterogeneous Fenton oxidation and anaerobic biological process, in the treatment of real British Gas/Lurgi coal gasification wastewater (BGLCGW). The Fenton oxidation process using CFA/sewage sludge carbon composite had increased efficiency in BGLCGW treatment over wide pH range. Moreover, it is worth noting that the system was proved to be even 30 times reusable, and the treated wastewater had increased biodegradability. This facilitated the subsequent biological process. At the same time, the heterogeneous Fenton oxidation process notably improved effluent quality and significantly enhanced the anaerobic granular sludge properties. This, in turn, contributed to a high efficiency and stability of the ecosystem inside the bioreactor. By using this integrated process a COD removal efficiency of 75% and a total phenols (TPh) removal efficiency of 86% were achieved. This performance was approximately four times higher than that of a single anaerobic process at 12 h. Furthermore, the aerobic biodegradation of BGLCGW was enhanced by this integrated process. Indeed, the corresponding TPh and COD concentrations met the water reuse standard in the subsequent aerobic treatment of the effluent. Therefore, this integrated process was found to be suitable for engineering application, due to its stability, efficiency, and economic viability.

2.3. Combined and alternative advanced oxidation mechanisms

Several systems that employ combined advanced oxidation mechanisms have also been proposed:

The foremost alternative mechanisms applied involve the combination of photocatalysis and Fenton or Fenton-like. Sun and Zhang [65] prepared $BiVO_4$-loaded FA cenospheres (BFACs) photocatalysts by using the modified MOD method. The photocatalytic efficiency of the composite catalysts BFACs, evaluated by MO and phenol photodegradation in aqueous solutions under visible light irradiation, was much higher than that of pure $BiVO_4$. Indeed, much enhanced phenol removal efficiency was further achieved with photodegradation assisted by Fenton process (i.e., H_2O_2 reagent) to the advanced oxidation procedure. The photocatalysts BFACs exhibited enhanced stability and preserved a high MO photocatalytic efficiency during successive recycling. Furthermore, Visa et al. [66] produced a novel composite photocatalyst composed of FA and tungsten oxide, via hydrothermal synthesis. This catalyst was used as substrate for the advanced oxidation of wastewater loaded with complex pollutants deriving from textile industry. The treatment process proposed consisted of a single step process that was combining adsorption and photocatalysis. The photocatalytic properties and the adsorption capacity of the produced photocatalyst were evaluated using wastewater containing two dyes (Bemacid Rot and Bemacid Blau) and one heavy metal ion Cu^{2+}. Enhanced photocatalytic efficiency was determined when using the composite catalyst in the combined photocatalytic and adsorption process. Additionally, the results of the combined process were compared with those of the individual processes. It is noteworthy that the introduction of H_2O_2 substantially enhanced the removal efficiencies for both dyes. Bansal and Verma [67] used novel composite clay beads mixed with foundry sand (FS)/FA as support materials for TiO_2 catalyst fixation and also as iron source. A synergistic effect for the cephalexin (antibiotic) degradation was identified: the in situ iron generation induced a dual photo-Fenton and photocatalytic effect in the same treatment unit. The composite beads (i.e., FS/FA/TiO_2) achieved a photodegradation activity of 89% at optimized conditions, whereas the binary photocatalyst mixtures exhibited lower efficiencies. Specifically, FS/TiO_2 had 79% and FA/TiO_2 had 81% photocatalytic efficiency. The usefulness of the produced catalysts in real-scale applications was underlined by their reusability after 35 cycles. Mineralization of the pollutant was validated by a COD decrease (82%), accompanied with the generation of various anions. In another study of Bansal and Verma [68], an Fe/TiO_2 composite photocatalyst was developed, to combine the synergistic effect of both photocatalysis and photo-Fenton, for minimizing the treatment time for PEN degradation. Specifically, they combined FA (iron source), waste FS, and TiO_2, in either suspended or supported form. Both a reduction in treatment time from 90 to 30 min and also a 49% synergy in slurry mode for PEN degradation were achieved. The first-order rate constant (k) was substantially increased for the dual process along with the treatment time reduction. Interestingly, the synergistic effect was validated by achieving a threefold increase in k when employing the novel Fe-TiO_2 composite photocatalyst for PEN degradation. The catalyst reusability after 45 cycles was confirmed by the detection of TiO_2 and iron onto the composite surface. The PEN mineralization was confirmed by COD and total organic carbon (TOC) reductions, accompanied with several anions generation. Moreover, Jia et al. [69] investigated several types of modified FA regarding their advanced oxidation ability. They used an orthogonal test and single factor analysis to identify the effect of several experimental parameters and their optimal level combination in photo-Fenton procedure. The acid-modified FA exhibits a great synergistic effect in the AOP. For papermaking effluents treatment, when applying the method without wastewater pH regulation, the optimal reaction conditions were: 45 min reaction time, 34 g/L FA dosage, and 8.8 mmol/L $FeSO_4{\cdot}7H_2O$ dosage. In these conditions, the COD removal efficiency reached 71.72%. Furthermore, Benjelloun et al. [70] investigated the Fe-FAC catalytic activity in Crystal Violet (CV) wet oxidation by using H_2O_2. The effect of some significant parameters, such as dye concentration, catalyst dosage, precursor loading, pH, temperature, and the initial H_2O_2 concentration, was also investigated. The Fe-FAC/H_2O_2 procedure enhanced the CV removal under optimal conditions. Visa and Duta [71] proposed modified FA mixed with TiO_2 photocatalyst as a viable option for simultaneous removal of dyes and heavy metals. They optimized the conditions for treating synthetic wastewaters containing MO and Cd. For a cost-effective dye removal process, further tests were done, replacing the catalyst with a (photo)Fenton system. The optimized technological parameters (contact time, amounts of FA and Fe^{2+}/H_2O_2) allowed to reach removal efficiencies up to 88% for the heavy metal and up to 70% for the dye. The adsorption mechanisms and the process kinetics were discussed considering the possibility of in situ generation of the Fenton system due to the FA beneficial composition. In another study of Visa et al. [72], a composite photocatalyst from TiO_2 and FA was developed in mild hydrothermal conditions. Subsequently, the composite photocatalyst was utilized for the advanced oxidation of the wastewater with multiple pollutants. The photocatalytic efficiency was evaluated on synthetic solutions containing sodium dodecylbenzenesulfonate (surfactant), copper (a heavy metal cation), and MO (dye), under simulated solar radiation and UV. Comparative experimental results recorded in systems with and without Fenton reagent (H_2O_2) exhibited a substantial increase in MO degradation efficiency for ternary, binary, and one pollutant(s) solutions. Using the composite catalyst under both UV and simulated solar radiation, the heterogeneous process was more efficient than homogeneous photocatalysis.

Some other combined mechanisms used in advanced oxidation utilize ultrasonic (US) or microwave (MW) irradiation to enhance the photocatalytic efficiency of the system. Wei et al. [73] investigated the levofloxacin degradation in a combined system consisted of US/FA/H_2O_2. The influence of FA loading, levofloxacin initial concentration, H_2O_2 concentration, and pH on the degradation efficiency was evaluated. Levofloxacin photodegradation was substantially promoted in the ternary system US/FA/H_2O_2, when comparing with the sole process (i.e., sonolysis, Fenton) as well as the binary systems FA/H_2O_2 and US/H_2O_2. The degradation efficiency reached 99.12%, whereas TOC removal efficiency attained just 17.37%, under the optimal conditions: 15.0 mmol/L H_2O_2 concentration, pH = 7.16, 325 W US power, 20 mg/L levofloxacin, 1.5 g/L FA addition, and 160 min treatment time. Li et al. [74] investigated the combination of US irradiation and Fenton-like reagent effectiveness for the degradation of Acid brown 348 in aqueous solution. Effects of the reaction conditions on the Acid brown 348 removal were observed under ultrasound irradiation. The best removal ratio was 96% under the optimal conditions: pH = 2.5, 2.5 g/L FA dosage, 5.0 mM H_2O_2, 50 mg/L dye initial concentration, 40°C, 140 min reaction time, and 40 kHz US frequency. The wastewater from the factory was treated first by activated carbon absorption and then degraded with ultrasound/FA/H_2O_2. The CODCr removal efficiency of dye wastewater was 95%. Al-Hamadani et al. [75] examined the feasibility of using two types of FA as a low-cost catalyst to enhance the US degradation of ibuprofen (IBP) and sulfamethoxazole (SMX). Two FAs, from Belews Creek (BFA), a power station in North Carolina, and Wateree Station (WFA), a power station in South Carolina, were used. The results showed that higher than 99% removal of IBP and SMX was achieved within 30 and 60 min of sonication respectively, at 580 kHz and pH = 3.5. Moreover, the order for removal of IBP and SMX, in terms of frequency, was 580 kHz > 1,000 kHz > 28 kHz, and in terms of pH, was 3.5 > 7 > 9.5. WFA showed significant enhancement in the removal of IBP and SMX, which reached >99% within 20 and 50 min, respectively, at 580 kHz and pH = 3.5. This was presumably because WFA contains more SiO_2 than BFA, which can enhance the formation of OH radicals during sonication. Additionally, WFA has finer particles than BFA, which can increase the adsorption capacity in removing IBP and SMX. Overall, it was shown that WFA combined with US has the potential for treating organic pollutants such as IBP and SMX in water and wastewater. Bečelić-Tomin et al. [76] investigated the possibility of FA and pyrite ash applications as Fenton catalysts in the advancement of the MW/H_2O_2 treatment in the RhB decolorization process. At the same time, a comparison of the influence of these heterogeneous catalysts with the homogeneous Fenton catalyst on the decolorization process was conducted. The influence of the catalyst was tracked in previously optimized MW/H_2O_2

conditions: 0.2 mM RhB concentration, 80 mM H_2O_2 concentration, pH = 3.2, 85°C temperature, and 300 W power. Under these conditions, an efficiency of 99.5% was achieved after 30 min of reaction. The same efficiency was achieved through the application of MW/Fe^{2+}/H_2O_2 and MW/pyrite ash/H_2O_2 after only 10 min of reaction. Li et al. [77] investigated the feasibility of FA for enhanced degradation of an azo dye AO7 under US irradiation. The decolorization efficiency for AO7 by the combined process could reach 76.7%, while US process alone only removed 3.8% of AO7 within 60 min. A synergetic effect between FA and US irradiation was firstly observed. The decolorization of AO7 fitted the first-order rate kinetics, and the $k1$ was 0.0246 min^{-1} for the combined process. Radical quenching experiment by iso-propanol revealed that 24.8% of AO7 decolorization could be attributed to hydroxyl radicals, indicating that the contribution of hydroxyl radicals was not as significant as expected.

Ma et al. [78] developed an efficient and economical catalyst and scrutinized its capacity for 2-chlorophenol degradation in wastewater via ozonation oxidation by using an ozone batch reactor. The catalyst was directly prepared by sawdust and FA reuse after saturated nickel ions adsorption from wastewater. A synergistic effect between FA and sawdust was found. Specifically, FA plays the role of the basic framework, having a high specific surface area, and the sawdust admixture acts as a pore-former, improving the porous morphology of the catalytic material. The catalyst addition improved the ozonation reaction efficiency evaluated in 2-chlorophenol degradation at a 2:1 liquid–solid ratio and at pH = 7. The kinetic study demonstrated that the reaction followed a first-order model, with a 267% increase in the rate constant of 2-chlorophenol degradation, compared with the ozonation solely at pH = 7.0 with 5 mmol/L concentration. He et al. [79] studied the ozonolysis of oleic acid (OA). Specifically, they evaluated the impact of FA in heterogenous reaction through the comparison of ozone oxidation reaction kinetics between the OA thin film and OA-coated FA, observed by in situ vacuum Fourier-transform infrared. The OA component of the two samples could be gradually consumed and converted to some products containing hydroxyl and ester groups during the reactions through the changing trends of the infrared spectrum. The ozonolysis reaction rate constant of OA-coated FA is nearly double to the OA thin film. Rapid reaction rate of the FA sample is due to the larger catalytic surface area and a more valid catalytic effect compared with the OA thin film. This demonstrates that FA often easily leads to secondary organic aerosols, when it is united with unsaturated organic acids and exposed to the ozone oxidation environment.

Several works are destined toward the synthesis of novel electrocatalysts that can be used in AOPs. Zhuang et al. [80] developed a novel catalytic particle electrode (CPE) from CFA and waste rice straw. CFA was used to enhance the electro-Fenton AOP efficiency for wastewater that contains actual azo dyes. The produced CPE were reported to have superb electrocatalytic activity and substantially improved pollutant removal performance at approximately neutral pH. Specifically, a 73.5% COD and 90.5% color removal was achieved, which allowed the discharge criteria to be met. Moreover, the combination of CPE with electro-Fenton improved the wastewater biodegradability in terms of toxicity, 5-day biochemical oxygen demand/COD, and resazurin dehydrogenase activity. Thirumalai et al. [81] focused on ZnO photocatalyst modification via hydrothermal decomposition method using FA. The produced FA-ZnO exhibited improved photocatalytic efficiency for the degradation of three different azo dyes (Trypan Blue, Reactive Orange 4, and RhB) and methanol. Indeed, the improved FA-ZnO hydrophobic effect contributed to its self-cleaning property.

Some other works are dedicated to more complicated combinations of advanced oxidation mechanisms and wastewater treatment processes such as persulfate oxidation, catalytic oxidation, coagulation, and acidification. In particular, Nachiappan et al. [82] proposed a novel heterogeneous FA-activated persulfate oxidation for the degradation of a pharmaceutical effluent. By this procedure, an inexpensive and difficult to degrade waste by-product such as FA exhibited the potential to decompose and mineralize the effluent effectively. Interestingly, two different FAs, one with high iron content (FA1) and another with less iron (FA2) were employed as activator. The effect of reaction time, temperature, agitation rate, initial pH, and dose of FA on COD and TOC reduction was analyzed for both FA1 and FA2. At lower temperatures, FA1 catalyzed persulfate oxidation efficiently due to the presence of high % iron. On the other hand, at higher temperatures, both FA1 and FA2 performed in similar way, as heat appeared to be the activator in persulfate oxidation. Maximum degradation was achieved at highly acidic conditions, and the degradation decreases with increase in pH up to 7.0, beyond which little increase in degradation was observed. Increase in FA dose enhanced the degradation. The effluent treated using FA1 produced less toxic wastewater than FA2. Liu and Yuan [83] investigated the treatment efficiency of high concentrated drilling wastewater, with COD concentration of 14,460.0 mg/L from Huabei oil field, by using the combined processes, with acidification, coagulation, catalytic oxidation, and adsorption. A Ni-based catalyst was carefully developed, and the effects of calcium hypochlorite ($Ca(ClO)_2$) dosage, Ni-based catalyst dosage, pH value, and reaction time on COD and color removal efficiency were studied. Under the optimal conditions of 4.4 g/L $Ca(ClO)_2$ dosage, 1.6 g/L Ni-based catalyst dosage and pH = 4, the COD concentration decreased to 403.5 mg/L. For advanced treatment of the drilling wastewater, the adsorption method with modified FA was used. Under the optimal conditions, the COD concentration declined to 139.9 mg/L, and the quality of final effluent met the GB8978-1996 standards of wastewater discharge.

A comprehensive overview of the literature review conducted is provided in Table 1, summarizing Advanced oxidation methods/mechanisms, pollutants oxidized, FA-based catalytic agents and main results.

3. Conclusions

From the extensive recent literature review carried out, the significance of advanced oxidation in wastewater treatment using FA-based catalysts was underlined. Several catalytic systems with sophisticated (nano)structures, composed of two or more constituents, exhibited the highest oxidation (degradation) efficiencies.

Furthermore, catalytic systems that could be used in combined advanced oxidation mechanisms also showed

Table 1
An overview of the literature review

Advanced oxidation process	Oxidized pollutant	Fly ash (FA)-based catalytic agent	Main results	References
Photocatalysis	Acid Red 1	Class C and Class F FAs	Degradation rates up to 95%	[23]
Photocatalysis	*o*-Chlorophenol	Modified FA and TiO_2 nanoparticles	Removal efficiency by mixture of modified FA and TiO_2 increased to 98.9%, compared to the one of pristine TiO_2 that was 78.7%	[24]
Photocatalysis	Phenol, imidacloprid and dichloroacetic acid	Composite mixture of FA and TiO_2	Complete degradation of dichloroacetic acid. Imidacloprid and phenol removal of 90% and 56%, respectively	[25]
Photocatalysis	Diclofenac sodium solution	FA/TiO_2	Degradation efficiency above 70% even after 6 cycles	[26]
Photocatalysis	Bemacid Blau (BB) and Bemacid Rot (BR)	$FA\text{-}TiO_2$ nanocomposite	High removal efficiencies, above 90%	[27]
Photocatalysis	Methylene blue, surfactant dodecylbenzenesulfonate (SDBS) and copper cation	$TiO_2\text{-}FA$ composite	FA suitable substrate for efficient adsorption and photodegradation of complex pollutants. FA-based composites efficient materials for up-scalable processes	[28]
Photocatalysis	• Methylene blue • Antibacterial activity against *Escherichia coli*	FA/TiO_2 nanofibers	Enhanced photocatalytic and antibacterial properties	[29]
Photocatalysis	Methylene blue (MB)	TiO_2 nanosheets on coal FA microspheres	Decolorization rates above 43%	[30]
Photocatalysis	Rhodamine B (RhB) aqueous solution	Mesoporous TiO_2-coated $ZnFe_2O_4$ nanocomposite loading on activated FA cenosphere	RhB removal rate up to 97.1	[31]
Photocatalysis	Methyl orange (MO)	FA supported $g\text{-}C_3N_4/N\text{-}TiO_2$	MO degradation up to 72% under visible light. Seven times reusability with degradation >68%	[32]
Photocatalysis	Tetracycline hydrochloride	$H_3PW_{12}O_{40}\text{-}CS/TiO_2$/fly ash cenospheres (HPW-CS/TiO_2/FACS)	HPW-CS/TiO_2/FACS showed higher photocatalytic activity than TiO_2/FACS	[33]
Photocatalysis	Methylene blue	$Ag_3PO_4/ZnFe_2O_4$/FACs	Retention of high photocatalytic activity after five times of recovery	[34]
Photocatalysis	Rhodamine B	Ag@AgCl-doped TiO_2/FA cenospheres	Rhodamine B degradation nearly 100% within 120 min under visible light	[35]
Photocatalysis	Dimethylformamide (DMF)	V-doped TiO_2/FA cenospheres	Degradation rates up to 88.2%	[36]
Photocatalysis	Scarlet 4BS	V-TiO_2/FA	Degradation rates up to 98.7%	[37]
Photocatalysis	Methylene blue	Pt–TiO_2 films supported on hydroxylated FA cenospheres	Enhanced photocatalytic efficiency	[38]
Photocatalysis	Bemacid Red (BR), Bemacid Blue (BB)	FA–TiO_2 composite	Removal efficiencies up to 93% for BR and 77% for BB	[39]
Photocatalysis	Ciprofloxacin	Poly *o*-phenylenediamine (PoPD)-modified porous TiO_2/FA cenospheres	Degradation rates up to 71.36%	[40]

Advanced oxidation process	Oxidized pollutant	Fly ash (FA)-based catalytic agent	Main results	References
Photocatalysis	Rhodamine B (RhB)	Hybrid carbonized chitosan and Fe-N-codoped TiO_2 on FA cenospheres	Degradation with Fe-N-TiO_2/FAC-Cts about 1.5 and 2.09 times higher than with Fe-N-TiO_2/FAC and N-TiO_2/FAC, respectively	[41]
Photocatalysis	Tetracycline, oxytetracycline, ciprofloxacin, tetracycline hydrochloride, and chloromycetin	Transition metal ion–poly-*o*-phenylenediamine/TiO_2/FA cenospheres	Photodegradation rates up to 71.7%	[42]
Photocatalysis	Tetracycline (TC), oxytetracycline (OTC) and ciprofloxacin (CIP)	POPD/TiO_2/FA cenospheres	Degradation rates up to 77%	[43]
Photocatalysis	Methyl orange (MO)	N, S codoped-TiO_2/FA beads composite	Degradation rate up to 65%	[44]
Photocatalysis	Methylene blue (MB)	ZnS-enwrapped-amine functionalized FA nanocomposite	Catalytic activity of FA-supported ZnS higher to that of bare ZnS nanoparticles	[45]
Photocatalysis	Congo red dye and pathogenic bacteria (*Staphylococcus aureus* and *Escherichia coli*)	ZnS/SnS/functionalized FA	Congo red dye degradation within 150 min using 10 mg of photocatalyst	[46]
Photocatalysis	Methylene blue (MB)	Ag/ZnO/FA nanocomposite	High photocatalytic and antibacterial capacity with good reusability	[47]
Photocatalysis	Danofloxacinmesylate	CdS/magnetic FA cenospheres	Degradation rates up to 76.2%	[48]
Photocatalysis	Enrofloxacin hydrochloride	TiO_2 photocatalyst based on magnetic floating FA cenospheres	Removal efficiency up to 75.32%	[49]
Photocatalysis	Rhodamine B	BiOBr/BiOI hierarchical microspheres on FA cenospheres	BiOBr/BiOI/FACs reached 70 % pollutant absorption, leading to highest degradation rates	[50]
Photocatalysis	Methylene blue (MB)	CeO_2–$BiVO_4$/FA composites	Enhanced photocatalytic activity and reusability for more than five times	[51]
Photocatalysis	Methylene blue (MB)	FA-cenospheres supported $BiVO_4$	Excellent photocatalytic activity with a first-order reaction rate constant ($k1$) 2.5 times higher than that with pure $BiVO_4$	[52]
Photocatalysis	Methylene blue (MB)	Pt–BiVO4/FA composite	Highest $k1$ for the composite with 2wt. % Pt	[53]
Photocatalysis	Methylene blue (MB)	FA-based geopolymer	Degradation rates up to 92.79%	[54]
Fenton	Phenols and aldehydes	FA	Rapid reaction with pollutants, effectively reducing the subsequent processing load	[55]
Fenton combined process	Dioctyl phthalate (DOP)	FA	Removal efficiency up to 83.21%	[56]
Fenton	Reactive Blue 181 (RB 181)	FA	90% removal efficiency	[57]
Fenton-like	*p*-Nitrophenol (*p*-NP) wastewater	HNO_3-modified coal FA (HFA)	Favorable HFA stability and reusability (nine times with >91% *p*-NP removal	[58]
Heterogeneous Fenton-like	*p*-Nitrophenol (*p*-NP)	Fe_2O_3/coal FA	64.3% *p*-NP removal	[59]
H_2O_2	Phenol wastewater	FA	99.46% removal rate	[60]

Continued

Table 1 *Continued*

Advanced oxidation process	Oxidized pollutant	Fly ash (FA)-based catalytic agent	Main results	References
Fenton-like	Reactive blue 182 dye (RB182)	Iron-modified FA	93% RB182 removal, under the optimal conditions	[61]
Fenton-like	Reactive blue 19 dye	Iron-modified FA	Degradation up to 97% and reusability	[62]
Fenton-like	*n*-Butyl xanthate	FA	Over 96.66% COD removal	[63]
Fenton	British Gas/Lurgi coal gasification wastewater (BGLCGW)	Coal FA/sewage sludge carbon composite and anaerobic biological process	Efficient pollutant removal performance at 30 reusability runs	[64]
Photocatalysis/Fenton	Methyl orange (MO) and phenol	$BiVO_4$-loaded FA cenospheres	Photodegradation of MO over BFACs 50% higher than that over pure $BiVO_4$	[65]
Photocatalysis/H_2O_2	Bemacid Blau (BB) and Bemacid Rot (BR)	FA–WO_3 composites	Removal efficiencies up to 70%	[66]
Photocatalysis and photo-Fenton	Cephalexin (CEX)	TiO_2 immobilized novel clay beads with waste FA/foundry sand (FA/FS/TiO_2)	Around 89% photodegradation (UV) after 4 h, under optimized conditions	[67]
Photocatalysis and photo-Fenton	Pentoxifylline (PEN)	Novel Fe-TiO_2 composite	Two- to sixfolds decrease in half-life of PEN. Stability and activity of catalyst even after 45 recycles	[68]
Photo-Fenton	Papermaking wastewater	Modified FA	COD removal efficiency up to 71.72%	[69]
Hydrogen peroxide (H_2O_2)	Crystal Violet (CV)	Fe/FA catalyst	100% decolorization of 30 ppm initial CV concentration after < 30 min	[70]
Photo-Fenton	Methyl-orange (MO)	FA/TiO_2	Removal efficiencies up to 88%	[71]
Photocatalysis/H_2O_2	Methyl orange	FA/TiO_2	Degradation rates up to 92%	[72]
Sonocatalysis/H_2O_2	Levofloxacin (LF)	FA	Removal efficiency up to 99.12%	[73]
Sonocatalytic/Fenton-like	Acid Brown 348	FA	Removal efficiency up to 96%	[74]
Sonocatalysis	Ibuprofen (IBP) and sulfamethoxazole (SMX)	Two types of FA	Enhanced removal rate at 580 kHz	[75]
Microwave/Fenton	Rhodamine B	FA	99.5% removal efficiency	[76]
Sonocatalysis	Acid Orange 7 (AO7)	FA	Decolorization efficiency of AO7 up to 76.7%	[77]
Catalytic ozonation	2-Chlorophenol	FA and sawdust	Significant improvement in the removal efficiency	[78]
Ozonolysis	Oleic acid (OA)	Oleic acid-coated FA	Ozonolysis reaction rate of OA-coated FA is nearly double to the OA thin film	[79]
Electro-Fenton	Azo dyes containing wastewater	Waste rice straw-coal FA composite	73.5% COD and 90.5% color removal efficiencies	[80]
Photocatalytic, electrocatalytic, and self-cleaning	Reactive Orange 4, Rhodamine B, and Trypan Blue	FA-supported ZnO nanorods	Stable and reusable catalyst	[81]
Persulfate oxidation	Real pharmaceutical effluent	Two types of Fe-containing FA	FA drastically reduced the apparent degradation activation energy	[82]
Catalytic oxidation	High concentrated drilling wastewater	Ni/FA	Enhanced COD and color removal efficiency at optimal conditions	[83]

enhanced degradation efficiencies and applicability to real-scale applications.

Future research works that investigate the synergy between traditional and industrial wastewater treatment procedures (e.g., absorption and filtration) and advanced oxidation would be beneficial for further enhancing the industrial applicability of advanced oxidation.

References

[1] J.R. Alvarez-Corena, J.A. Bergendahl, F.L. Hart, Advanced oxidation of five contaminants in water by UV/TiO_2: reaction kinetics and byproducts identification, J. Environ. Manage., 181 (2016) 544–551.

[2] Z. Frontistis, M. Kouramanos, S. Moraitis, E. Chatzisymeon, E. Hapeshi, D. Fatta-Kassinos, N.P. Xekoukoulotakis, D. Mantzavinos, UV and simulated solar photodegradation of 17α-ethynylestradiol in secondary-treated wastewater by hydrogen peroxide or iron addition, Catal. Today, 252 (2015) 84–92.

[3] E. Giannakopoulos, E. Isari, K. Bourikas, H.K. Karapanagioti, G. Psarras, G. Oron, I.K. Kalavrouziotis, Oxidation of municipal wastewater by free radicals mechanism. A UV/Vis spectroscopy study, J. Environ. Manage., 195 (2017) 186–194.

[4] E. Katsika, A. Moutsatsou, V. Karayannis, M. Volioti, D. Tsoukleris, Synthesis and characterization of lignite fly ash ceramic substrates coated with TiO_2 slurry, and evaluation in environmental applications, J. Aust. Ceram. Soc., (In press) doi:10.1007/s41779-018-0201-8.

[5] K. Loganathan, Ozone-based advanced oxidation processes for the removal of harmful algal bloom (HAB) toxins: a review, Desal. Wat. Treat., 59 (2017) 65–71.

[6] C.A. Papadimitriou, P. Samaras, A.I. Zouboulis, M. Yiangou, G.P. Sakellaropoulos, Role of extracellular polymeric substances on two biological reactors performance treating phenol, Environ. Eng. Manage. J., 16 (2017) 1843–1852.

[7] S. Ameta, R. Ameta, Advanced Oxidation Processes for Wastewater Treatment: Emerging Green Chemical Technology, Elsevier Science, London, 2018.

[8] N.C. Shang, Y.H. Yu, H.W. Ma, C.H. Chang, M.L. Liou, Toxicity measurements in aqueous solution during ozonation of mono-chlorophenols, J. Environ. Manage., 78 (2006) 216–222.

[9] J.J. Pignatello, E. Oliveros, A. MacKay, Advanced oxidation processes for organic contaminant destruction based on the Fenton reaction and related chemistry, Crit. Rev. Env. Sci. Technol., 36 (2006) 1–84.

[10] M.N. Chong, B. Jin, C.W.K. Chow, C. Saint, Recent developments in photocatalytic water treatment technology: a review, Water Res., 44 (2010) 2997–3027.

[11] S. Malato, P. Fernández-Ibáñez, M.I. Maldonado, J. Blanco, W. Gernjak, Decontamination and disinfection of water by solar photocatalysis: recent overview and trends, Catal. Today, 147 (2009) 1–59.

[12] M. Pera-Titus, V. García-Molina, M.A. Baños, J. Giménez, S. Esplugas, Degradation of chlorophenols by means of advanced oxidation processes: a general review, Appl. Catal., B, 47 (2004) 219–256.

[13] E. Neyens, J. Baeyens, A review of classic Fenton's peroxidation as an advanced oxidation technique, J. Hazard. Mater., 98 (2003) 33–50.

[14] V. Karayannis, K. Moustakas, A. Vatalis, P. Sapalidis, A. Domopoulou, Advanced oxidation of industrial effluents under microwave irradiation: state of the art, Desal. Wat. Treat., 91 (2017) 138–145.

[15] K. Soutsas, V. Karayannis, I. Poulios, A. Riga, K. Ntampegliotis, X. Spiliotis, G. Papapolymerou, Decolorization and degradation of reactive azo dyes via heterogeneous photocatalytic processes, Desalination, 250 (2010) 345–350.

[16] K. Ntampegliotis, A. Riga, V. Karayannis, V. Bontozoglou, G. Papapolymerou, Decolorization kinetics of Procion H-exl dyes from textile dyeing using Fenton-like reactions, J. Hazard. Mater., 136 (2006) 75–84.

[17] A. Riga, K. Soutsas, K. Ntampegliotis, V. Karayannis, G. Papapolymerou, Effect of system parameters and of inorganic salts on the decolorization and degradation of Procion H-exl dyes. Comparison of H_2O_2/UV, Fenton, UV/Fenton, TiO_2/UV and TiO_2/UV/H_2O_2 processes, Desalination, 211 (2007) 72–86.

[18] I. Fatimah, I. Sumarlan, T. Alawiyah, Fe(III)/TiO_2-montmorillonite photocatalyst in photo-Fenton-like degradation of methylene blue, Int. J. Chem. Eng. 2015 (2015) 9 pages, doi:10.1155/2015/485463.

[19] N. Philippidis, S. Sotiropoulos, A. Efstathiou, I. Poulios, Photoelectrocatalytic degradation of the insecticide imidacloprid using TiO_2/Ti electrodes, J. Photochem. Photobiol., A, 204 (2009) 129–136.

[20] E. Katsika, A. Moutsatsou, V. Karayannis, A. Ntziouni, Preparation and characterization of lignite ashes coated with TiO_2 for environmental application, J. Chem. Technol. Metall., 52 (2017) 940–949.

[21] Y. Chen, J. Lu, H. Han, J. Li, Y. Chen, Advances in environmental material utilization of fly ash, Chem. Bull., 76 (2013) 811–821.

[22] S. Wang, Application of solid ash based catalysts in heterogeneous catalysis, Environ. Sci. Technol., 42 (2008) 7055–7063.

[23] P.V.S. Giri Babu, G. Swaminathan, Comparative study on synergetic degradation of a reactive dye using different types of fly ash in combined adsorption and photocatalysis, J. Inst. Eng. (India) A, 97 (2016) 239–246.

[24] M. Malakootian, A. Mesdaghinia, S. Rezaei, Photocatalytic removal of o-chlorophenol by using a mixture of modified fly ash and TiO_2 nanoparticles, J. Kerm. Univ. Med. Sci., 24 (2017) 147–158.

[25] L. Andronic, L. Isac, S. Miralles-Cuevas, M. Visa, I. Oller, A. Duta, S. Malato, Pilot-plant evaluation of TiO_2 and TiO_2-based hybrid photocatalysts for solar treatment of polluted water, J. Hazard. Mater., 320 (2016) 469–478.

[26] J. Shi, H. Ai, X. Wang, M. Fu, Photocatalytic degradation of diclofenac sodium over the photocatalyst of TiO_2/CFA, Huanjing Kexue Xuebao/Acta Sci. Circum., 34 (2014) 370–376.

[27] M. Visa, L. Andronic, A. Duta, Fly ash-TiO_2 nanocomposite material for multi-pollutants wastewater treatment, J. Environ. Manage., 150 (2015) 336–343.

[28] M. Visa, L. Andronic, A. Enesca, Behavior of the new composites obtained from fly ash and titanium dioxide in removing of the pollutants from wastewater, Appl. Surf. Sci., 388 (2016) 359–369.

[29] P.S. Saud, B. Pant, M. Park, S.H. Chae, S.J. Park, M. Ei-Newehy, S.S. Al-Deyab, H.Y. Kim, Preparation and photocatalytic activity of fly ash incorporated TiO_2 nanofibers for effective removal of organic pollutants, Ceram. Int., 41 (2015) 1771–1777.

[30] X. Cui, J. Shi, Z. Ye, Z. Zhang, B. Xu, S. Chen, Layer-by-layer assembly and photocatalytic activity of titania nanosheets on coal fly ash microspheres, Int. J. Photoenergy, 2014 (2014) 10 pages, doi:10.1155/2014/823078.

[31] H. Fan, D. Chen, X. Ai, S. Han, M. Wei, L. Yang, H. Liu, J. Yang, Mesoporous TiO_2 coated $ZnFe_2O_4$ nanocomposite loading on activated fly ash cenosphere for visible light photocatalysis, RSC Adv., 8 (2018) 1398–1406.

[32] Z. Zhao, Y. Lei, W. Liu, J. Fan, D. Xue, Y. Xue, S. Yin, Fly ash cenospheres as multifunctional supports of g-C_3N_4 /N-TiO_2 with enhanced visible-light photocatalytic activity and adsorption, Adv. Powder Technol., 28 (2017) 3233–3240.

[33] J. Yang, M. Zhu, H. Chu, H. Zhou, Y. Xu, Preparation of HPW-CS/TiO_2/FACS photocatalysts for degradation of tetracycline hydrochloride, Mater. Technol., 32 (2017) 647–656.

[34] G. Hou, Y. Li, W. An, S. Gao, W. Zhang, W. Cui, Fabrication and photocatalytic activity of floating type Ag_3PO_4/$ZnFe_2O_4$/FACs photocatalyst, Mater. Res. Bull., 94 (2017) 263–271.

[35] S. Liu, J. Zhu, Q. Yang, P. Xu, J. Ge, X. Guo, Synthesis and characterization of cube-like Ag@AgCl-doped TiO_2/fly ash cenospheres with enhanced visible-light photocatalytic activity, Opt. Mater., 53 (2016) 73–79.

[36] X.M. Fan, C.H. Bai, G.H. Li, Z.Y. Xu, J.K. Sheng, Z.K. Guo, Study on photocatalytic degradation of DMF by V-Doped TiO_2/Fly ash cenosphere, Rengong Jingti Xuebao/J. Synth. Cry., 45 (2016) 736–742.

[37] Y. Zhao, X. Zhang, X. Zhao, L. Geng, Preparation and characterization of V-TiO_2/fly-ash cenospheres and its photocatalytic properties, Optoelectron. Adv. Mater. Rapid Commun., 7 (2013) 129–132.

[38] B. Wang, Z. Yang, H. An, J. Zhai, Q. Li, H. Cui, Photocatalytic activity of Pt-TiO_2 films supported on hydroxylated fly ash cenospheres under visible light, Appl. Surf. Sci., 324 (2015) 817–824.

[39] A. Duta, M. Visa, Simultaneous removal of two industrial dyes by adsorption and photocatalysis on a fly-ash-TiO_2 composite, J. Photochem. Photobiol., A, 306 (2015) 21–30.

[40] P. Huo, M. Zhou, X. Yan, X. Liu, Z. Lu, R. Zhang, W. Shi, Y. Yan, Preparation of PoPD modified porous TiO_2/fly-ash cenosphere photocatalysts and their photocatalytic activity on ciprofloxacin antibiotics, Fresenius Environ. Bull., 23 (2014) 1860–1866.

[41] J. Song, X. Wang, Y. Bu, X. Wang, J. Zhang, J. Huang, R. Ma, J. Zhao, Photocatalytic enhancement of floating photocatalyst: layer-by-layer hybrid carbonized chitosan and Fe-N-codoped TiO_2 on fly ash cenospheres, Appl. Surf. Sci., 391 (2017) 236–250.

[42] X. Yu, X. Gao, Z. Lu, X. Liu, P. Huo, X. Liu, D. Wu, Y. Yan, Preparation and photodegradation properties of transition metal ion-poly-o-phenylenediamine/TiO_2/fly-ash cenospheres by ion imprinting technology, RSC Adv., 3 (2013) 14807–14813.

[43] Z. Lu, P. Huo, Y. Luo, X. Liu, D. Wu, X. Gao, C. Li, Y. Yan, Performance of molecularly imprinted photocatalysts based on fly-ash cenospheres for selective photodegradation of single and ternary antibiotics solution, J. Mol. Catal. A: Chem., 378 (2013) 91–98.

[44] J. Lv, T. Sheng, L. Su, G. Xu, D. Wang, Z. Zheng, Y. Wu, N, S co-doped-TiO_2/fly ash beads composite material and visible light photocatalytic activity, Appl. Surf. Sci., 284 (2013) 229–234.

[45] K. Kalpana, V. Selvaraj, Photodegradation and antibacterial studies of ZnS enwrapped fly ash nanocomposite for multipurpose industrial applications, RSC Adv., 5 (2015) 47766–47777.

[46] K. Kalpana, V. Selvaraj, Development of ZnS/SnS/A-FA nanorods at ambient temperature: binary catalyst for the removal of congo red dye and pathogenic bacteria from wastewater, J. Ind. Eng. Chem., 41 (2016) 105–113.

[47] H.J. Kim, M.K. Joshi, H.R. Pant, J.H. Kim, E. Lee, C.S. Kim, One-pot hydrothermal synthesis of multifunctional Ag/ZnO/fly ash nanocomposite, Colloids Surf., A, 469 (2015) 256–262.

[48] M. He, Z. Lu, W. Zhou, T. Chen, W. Shi, G. Che, P. Huo, Z. Zhu, X. Zhao, Y. Yan, A novel CdS photocatalyst based on magnetic fly ash cenospheres as the carrier: performance and mechanism, RSC Adv., 4 (2014) 60148–60157.

[49] Z. Lu, W. Zhou, P. Huo, Y. Luo, M. He, J. Pan, C. Li, Y. Yan, Performance of a novel TiO_2 photocatalyst based on the magnetic floating fly-ash cenospheres for the purpose of treating waste by waste, Chem. Eng. J., 225 (2013) 34–42.

[50] L. Lin, Y. Wang, M. Huang, D. Chen, Immobilization of BiOBr/BiOI hierarchical microspheres on fly ash cenospheres as visible light photocatalysts, Aust. J. Chem., 69 (2016) 119–125.

[51] J. Zhang, B. Wang, C. Li, H. Cui, J. Zhai, Q. Li, Synthesis of novel CeO_2-$BiVO_4$/FAC composites with enhanced visible-light photocatalytic properties, J. Environ. Sci., 26 (2014) 1936–1942.

[52] J. Zhang, H. Cui, B. Wang, C. Li, J. Zhai, Q. Li, Fly ash cenospheres supported visible-light-driven $BiVO_4$ photocatalyst: synthesis, characterization and photocatalytic application, Chem. Eng. J., 223 (2013) 737–746.

[53] J. Zhang, Preparation of novel Pt-$BiVO_4$/fly ash cenospheres composites with high photocatalytic performance, Adv. Mater. Res., 1010–1012 (2014) 216–219.

[54] Y. Zhang, L. Liu, Fly ash-based geopolymer as a novel photocatalyst for degradation of dye from wastewater, Particuology, 11 (2013) 353–358.

[55] H.C. Pang, H.Y. Fu, T.Z. Gao, Treatment of high concentration wastewater containing phenols and aldehyde from a small Phenolic resin plant, Adv. Mater. Res., 864–867 (2014) 1552–1555.

[56] L.P. Wang, X.Y. Li, X.M. Li, Dioctyl phthalate esters wastewater treatment by Fenton reagent/fly ash combined process, Adv. Mater. Res., 777 (2013) 122–126.

[57] D.S. Duc, Degradation of reactive blue 181 dye by heterogeneous Fenton technique using modified fly ash, Asian J. Chem., 25 (2013) 4083–4086.

[58] N. Wang, Q. Zhao, A. Zhang, Catalytic oxidation of organic pollutants in wastewater: via a Fenton-like process under the catalysis of HNO_3-modified coal fly ash, RSC Adv., 7 (2017) 27619–27628.

[59] N. Wang, J. Chen, Q. Zhao, H. Xu, Study on preparation conditions of coal fly ash catalyst and catalytic mechanism in a heterogeneous Fenton-like process, RSC Adv., 7 (2017) 52524–52532.

[60] J. Wang, H.J. Li, Q.K. Cheng, X.T. Yan, A.Q. Cao, Q.Y. Tan, Treatment of phenol wastewater with modified coal fly ash-Fenton reagent, Adv. Mater. Res., 955–959 (2014) 623–627.

[61] D.S. Dao, N. Van Nguyen, S.T. Le, H.K. Dieu Nguyen, H. Van Hoang, K.N. Truong, T.Q. Do, H. Yamada, Iron-Modified Fly Ash as Heterogeneous Fenton-Like Catalyst for Decolorization of Reactive Blue 182 Dye, In: J. Parker, Ed., Fly Ash: Properties, Analysis and Performance, Nova Science Publishers Inc, New York, 201, pp. 237–251.

[62] D.S. Duc, T. Le Hung, D.D. Khai, Degradation of reactive blue 19 dye in aqueous solution using iron-modified fly ash, Int. J. ChemTech. Res., 9 (2016) 533–538.

[63] S.H. Chen, D.Y. Du, Degradation of n-butyl xanthate using fly ash as heterogeneous Fenton-like catalyst, J. Cent. S. Univ., 21 (2014) 1448–1452.

[64] H. Zhuang, H. Han, S. Shan, Treatment of British Gas/Lurgi coal gasification wastewater using a novel integration of heterogeneous Fenton oxidation on coal fly ash/sewage sludge carbon composite and anaerobic biological process, Fuel, 178 (2016) 155–162.

[65] Y.X. Sun, J. Zhang, Photocatalytic degradation of methyl orange and phenol by $BiVO_4$-loaded fly ash cenospheres (FACs) composite, Adv. Mater. Res., 821–822 (2013) 471–475.

[66] M. Visa, C. Bogatu, A. Duta, Tungsten oxide – fly ash oxide composites in adsorption and photocatalysis, J. Hazard. Mater., 289 (2015) 244–256.

[67] P. Bansal, A. Verma, Synergistic effect of dual process (photocatalysis and photo-Fenton) for the degradation of Cephalexin using TiO_2 immobilized novel clay beads with waste fly ash/foundry sand, J. Photochem. Photobiol., A, 342 (2017) 131–142.

[68] P. Bansal, A. Verma, Novel Fe-TiO_2 composite driven dual effect for reduction in treatment time of pentoxifylline: slurry to immobilized approach, Mater. Design, 125 (2017) 135–145.

[69] X.F. Jia, W.N. Mai, X.R. Wang, J. Zhou, Advanced treatment on papermaking wastewater using photo-Fenton modified fly ash, Appl. Mech. Mater., 535 (2014) 230–236.

[70] Y. Benjelloun, A. Lahrichi, S. Boumchita, M. Idrissi, Y. Miyah, K. Anis, V. Nenov, F. Zerrouq, Removal of Crystal Violet by wet oxidation with H_2O_2 over an Iron oxide catalyst synthesized from Fly Ash, J. Mater. Environ. Sci., 8 (2017) 2259–2269.

[71] M. Visa, A. Duta, Methyl-orange and cadmium simultaneous removal using fly ash and photo-Fenton systems, J. Hazard. Mater., 244–245 (2013) 773–779.

[72] M. Visa, L. Isac, A. Duta, New fly ash TiO_2 composite for the sustainable treatment of wastewater with complex pollutants load, Appl. Surf. Sci., 339 (2015) 62–68.

[73] H. Wei, H. Yang, L. Zhao, K.B. Li, X.L. Yu, Enhancement of levofloxacin degradation in US/H_2O_2 system by addition of fly ash, Zhongguo Huanjing Kexue/China Environ. Sci., 34 (2014) 889–895.

[74] J.T. Li, R.J. Lan, B. Bai, Y.L. Song, Ultrasound-promoted degradation of acid brown 348 by Fenton-like processes, Asian J. Chem., 25 (2013) 2246–2250.

[75] Y.A.J. Al-Hamadani, C.M. Park, L.N. Assi, K.H. Chu, S. Hoque, M. Jang, Y. Yoon, P. Ziehl, Sonocatalytic removal of ibuprofen and sulfamethoxazole in the presence of different fly ash sources, Ultrason. Sonochem., 39 (2017) 354–362.

[76] M.R. Bečelić-Tomin, B.D. Dalmacija, D.D. Tomašević, J.J. Molnar, L.M. Rajić, Application of pyrite ash in the microwave Fenton process of decolorization of synthetic color solution, Hem. Ind., 67 (2013) 399–409.

[77] G. Li, W. Zhao, B. Wang, Q. Gu, X. Zhang, Synergetic degradation of Acid Orange 7 by fly ash under ultrasonic irradiation, Desal. Wat. Treat., 57 (2016) 2167–2174.

[78] W. Ma, P. Zong, Z. Cheng, B. Wang, Q. Sun, Adsorption and biosorption of nickel ions and reuse for 2-chlorophenol catalytic ozonation oxidation degradation from water, J. Hazard. Mater., 266 (2014) 19–25.

[79] X. He, C.B. Leng, Y.H. Zhang, A comparison of heterogeneous reaction kinetics of oleic acid thin film and oleic acid coated flyash with ozone using vacuum FTIR, Guang Pu Xue Yu Guang Pu Fen Xi/Spectr. Spectr. Anal., 36 (2016) 1576–1580.

[80] H. Zhuang, S. Shan, J. Guo, Y. Han, C. Fang, Waste rice straw and coal fly ash composite as a novel sustainable catalytic particle electrode for strengthening oxidation of azo dyes containing wastewater in electro-Fenton process, Environ. Sci. Pollut. Res., 24 (2017) 27136–27144.

[81] K. Thirumalai, S. Balachandran, M. Swaminathan, Superior photocatalytic, electrocatalytic, and self-cleaning applications of Fly ash supported ZnO nanorods, Mater. Chem. Phys., 183 (2016) 191–200.

[82] S. Nachiappan, K.P. Gopinath, Treatment of pharmaceutical effluent using novel heterogeneous fly ash activated persulfate system, J. Environ. Chem. Eng., 3 (2015) 2229–2235.

[83] Y. Liu, J. Yuan, Coagulate-catalytic oxidation treatment of high concentrated drilling wastewater, Chin. J. Environ. Eng., 7 (2013) 108–112.